Catalysis Science & Technology

PAPER

View Article Online
View Journal | View Issue

Cite this: *Catal. Sci. Technol.*, 2014, **4**, 516

Protodecarboxylation of carboxylic acids over heterogeneous silver catalysts†

Xiu Yi Toy, Irwan Iskandar Bin Roslan, Gaik Khuan Chuah and Stephan Jaenicke*

Received 6th August 2013,
Accepted 30th October 2013

DOI: 10.1039/c3cy00580a

www.rsc.org/catalysis

A heterogeneous supported Ag catalyst for the protodecarboxylation of aromatic carboxylic acids has been developed. Control of the metal particle size proved extremely important. The highest activity was achieved with a silver loading of 10 wt%, which had relatively big metal crystallites of 40 nm. It is inferred that the adsorption of the aromatic moiety requires terrace sites rather than edges or corners at the metal nanoparticle. The amphoteric support, γ-Al_2O_3, gave the most active catalysts. Oxygen coverage of the surface is essential for catalytic activity. A mechanism has been proposed with the critical steps (1) formation of a benzoyl anion by reaction with a base in the reaction medium, (2) binding of the anionic species at the Ag^+ surface sites with (3) extrusion of CO_2 and (4) proton transfer from another molecule of carboxylic acid, followed by desorption of the decarboxylated species and binding of the benzoate to the active site to complete the catalytic cycle. With 2-nitrobenzoic acid as substrate, the catalyst had a turnover frequency (TOF) of 216 h^{-1}. The catalyst showed good activity for benzoic acid with nitro, methoxy and halogen substituents at the *ortho*-position as well as for heteroaromatic carboxylic acids.

1. Introduction

Carboxylic acids are very attractive intermediates as they are readily available in a wide range of structures and at low cost.[1] Carboxylate groups can direct the regioselectivity in aromatic substitution reactions. Over the years, several catalytic methodologies involving carboxylic acids have been developed.[2,3] Protodecarboxylation, where surplus carboxylate groups are removed and replaced with hydrogen atoms, is an important reaction within this strategy. One of the earliest reports of a catalytic decarboxylation reaction was by Shepard *et al.* in 1930.[4] These authors obtained halogen-substituted furans by decarboxylating halogenated furancarboxylic acids with copper bronze as catalyst and a high boiling point base, quinoline. Nilsson's group decarboxylated 2-nitrobenzoic acid using a stoichiometric amount of copper(I) oxide.[5] The use of chelating agents such as 1,10-phenanthroline and 2,2′-bipyridine extended the scope of the reaction to a wider range of activated carboxylic acids such as benzoic acids with electron-withdrawing *ortho* substituents and heteroaromatic carboxylic acids.[6,7] In 2007, Gooßen and coworkers reported an excellent yield of 82% for the decarboxylation of 4-methoxybenzoic acid with the Cu_2O–phenanthroline–quinoline system.[8] This was a significant improvement over previously reported methodologies as only 10 mol% of the catalyst was required and decarboxylation of *para*-substituted aromatic carboxylic acids could be carried out at 170 °C instead of temperatures above 200 °C. With microwave heating, the reaction time could be shortened to 5–15 min.[9] Decarboxylative methodologies have also been used in the presence of D_2O to incorporate deuterium selectively into aromatic rings.[10] This gives access to valuable deuterium labelled compounds.

Besides the copper-based catalysts, precious metals were also reported to be active for protodecarboxylation of aromatic carboxylic acids. Dickstein *et al.*[11] used $Pd(CF_3COO)_2$ in the decarboxylation of 2,6-disubstituted benzoic acids. Although the reaction temperature was much lower, 70 °C, the substrates were limited to only benzoic acids with two *ortho* substituents, and 10 equivalents of trifluoroacetic acid were needed as additive. Sun and Zhao[12] found that $[(cod)Rh(\mu\text{-}OH)]_2$ gave yields of 71–99% for the decarboxylation of a small range of fluorinated benzoic acids. However, the use of an expensive Rh-based catalyst and the need for phosphine ligands to fine-tune its activity are drawbacks of this methodology. Subsequently, Nolan's group described a strongly basic *N*-heterocyclic carbene (NHC)–gold complex for decarboxylation reactions in the presence of toluene at 110 °C.[13] Larrosa and coworkers reported the use of *o*-Ph-C_6H_4(*t*-Bu)$_2$PAuCl, together with Ag_2O as additive and DMF as solvent, to mediate the decarboxylation of aromatic and heteroaromatic carboxylic acids.[14] By modulating the reactivity of the gold(I) species *via* ligands, the reaction could be carried out at temperatures as low as 60 °C. However, the gold(I)–aryl compounds obtained upon decarboxylation did

Department of Chemistry, National University of Singapore, Kent Ridge, Singapore 117543, Singapore. E-mail: chmsj@nus.edu.sg; Fax: +65 6779 1691; Tel: +65 6516 2918

† Electronic supplementary information (ESI) available: Fig. S1–S6, Table S1, estimation of surface Ag atoms. See DOI: 10.1039/c3cy00580a

not undergo protodemetallation. Due to the formation of these gold(I)–aryl species, a stoichiometric amount of the expensive Au(I)-based 'catalysts' was required.

Silver acetate together with a basic additive, K_2CO_3, was found to effectively decarboxylate a wide range of *ortho*-substituted benzoic acids at a relatively low reaction temperature of 120 °C.[15] The protodecarboxylation of *ortho*-substituted aromatic carboxylic acids by Ag_2CO_3 could be extended to heteroaromatic carboxylic acids by the addition of acetic acid.[16,17] These systems are preferred as they are simple silver salts without the need for ligands. However, their separation and recovery present problems as they are soluble in the heated reaction mixture. This can be overcome with heterogeneous catalysts which can be easily recovered after reaction, regenerated and reused.[18] In addition, surface properties such as acidity can be fine-tuned by an appropriate choice of the support to control activity and selectivity.[19,20] For instance, heterogeneous supported silver catalysts have been studied extensively and used in reactions such as oxidation,[21] reduction[22] and *N*-alkylation.[23] Thus, in the present study, we developed heterogeneous silver catalysts for the protodecarboxylation using 2-nitrobenzoic acid as a model compound (Scheme 1). The protodecarboxylation of other aromatic carboxylic acids was also investigated.

2. Experimental

All reagents were purchased from commercial sources and were used as received. Solvents were dried over 4 Å molecular sieves before use.

2.1 Preparation of supported silver catalysts

Catalysts with 10 wt% silver loading on the supports γ-Al_2O_3, MgO, ZnO_2, SiO_2, TiO_2 were prepared by wet impregnation.[24] In a typical preparation of 10 wt% Ag/Al_2O_3, 0.1570 g (0.9270 mmol) of $AgNO_3$ was dissolved in 15 ml of deionised water and 0.9 g of γ-Al_2O_3 was added. The mixture was stirred at 70 °C until almost dry. The slurry was dried in an oven at 100 °C overnight and calcined in air at 500 °C (heating rate 1 °C min^{-1}) for 1 h. In addition, catalysts with a silver loading of 5, 10, 15, and 20 wt% on γ-Al_2O_3 were prepared using the same method.

2.2 Preparation of unsupported silver catalysts

Unsupported silver and silver(I) oxide was prepared by thermal decomposition of commercial Ag_2CO_3 at a temperature of 400 °C and 200 °C for 1 h, respectively. The products are referred to as Ag (ex-Ag_2CO_3) and Ag_2O (ex-Ag_2CO_3). In addition, commercial Ag powder (Alfa Aesar, spherical silver particles, 365 mesh) and Ag_2O (Alfa Aesar, 99+%) were also used. These materials are referred to as Ag (commercial) and Ag_2O (commercial).

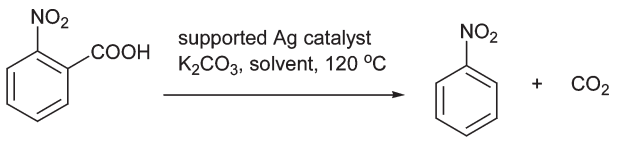

Scheme 1 Protodecarboxylation of 2-nitrobenzoic acid using supported Ag catalyst.

2.3 Characterization of alumina supported silver catalyst

Powder X-ray diffraction patterns were measured using a Siemens D5005 diffractometer equipped with a Cu anode and variable primary and secondary beam slits (scanning rate 0.02° s^{-1}, dwell time 1 s). The crystallite size of the silver particles was estimated from the full width at half maximum (FWHM) of the Ag (111) peak using the Scherrer equation.[25] Nitrogen adsorption and desorption isotherms were obtained at −196 °C with a TriStar 3000 (Micromeritics) porosimeter. The samples were degassed at 300 °C for 5 h prior to measurements. The specific surface area was calculated using the BET (Brunauer–Emmett–Teller) equation. Pore size distributions were calculated from the desorption branch of the isotherm by the BJH (Barrett–Joyner–Halenda) method. X-ray photoelectron spectra were measured on a VG Mark II Escalab using monochromated Mg K_α radiation (1253.6 eV) and a hemispherical electron analyzer at a constant transmission energy pass (50 eV). The binding energies were calibrated with reference to the C 1s peak at 284.6 eV. The relative surface concentration of Ag to Al was deduced from the Ag $3d_{5/2}$ and Al $3p_{3/2}$ peaks after correction using the atomic sensitivity factors provided by the manufacturer (ASF_{Ag} = 5.198, ASF_{Al} = 0.25). Transmission electron micrographs were obtained using a JEOL 2010. 5–10 mg of the powder sample were suspended in 2-propanol and sonicated for 15 min. A drop of the resultant slurry was deposited on a copper grid and dried overnight under ambient temperature before measurements.

2.4 Catalytic studies

The catalytic testing was carried out in a round-bottomed flask equipped with a Liebig condenser. Typically, 2-nitrobenzoic acid (2 mmol, 0.3342 g) and K_2CO_3 (0.3 mmol, 0.0415 g) were dissolved in 4 mL of *N*-methylpyrrolidone (NMP) as solvent and heated to 120 °C. After adding 10 mol% of the supported silver catalyst (0.2157 g catalyst containing 21.6 mg, 0.2 mmol Ag), the reaction was conducted under vigorous stirring. Aliquots were removed from the reaction mixture, filtered using a syringe filter and diluted 50 times with NMP. The diluted reaction mixture was then analyzed by HPLC (Shimadzu LC-10AT) with the UV detector set at λ = 254 nm. A reversed phase C-18 Shim-pack VP-ODS column (Shimadzu) was used as the stationary phase and the eluent, 50 : 50 : 0.4 (v/v/v) isopropanol : water : acetic acid, was delivered isocratically at a flow rate of 0.5 mL min^{-1}. Calibration curves were obtained for 2-nitrobenzoic acid and nitrobenzene.

3. Results and discussion

3.1 Catalyst characterization

The γ-Al_2O_3 and SiO_2-supported silver catalysts had high surface areas of 130 and 369 m^2 g^{-1}, respectively (Table 1). In

Table 1 BET surface area, pore volume and Ag crystallite size of the supported silver catalysts

Catalyst	Surface area (m^2 g^{-1})	Pore volume (cm^3 g^{-1})	Ag crystallite size[a] (nm)
10 wt% Ag/ZnO	8.2	0.05	114
10 wt% Ag/TiO_2	36	0.12	72
10 wt% Ag/MgO	90	0.14	63
10 wt% Ag/SiO_2	369	1.01	27
5 wt% Ag/γ-Al_2O_3	145	0.27	5
10 wt% Ag/γ-Al_2O_3	130	0.25	40
15 wt% Ag/γ-Al_2O_3	118	0.22	66
20 wt% Ag/γ-Al_2O_3	114	0.21	93
γ-Al_2O_3	148	0.27	n.a.
Ag (ex-Ag_2CO_3)[b]	0.2	0.003	—
Ag (commercial)	0.02	<0.001	—
Ag_2O (ex-Ag_2CO_3)[c]	0.9	0.003	—
Ag_2O (commercial)	0.3	<0.001	—

[a] From Scherrer equation. [b] Calcining Ag_2CO_3 at 400 °C for 1 h. [c] Calcining Ag_2CO_3 at 200 °C for 1 h.

contrast, the surface areas of the 10 wt% Ag/ZnO and 10 wt% Ag/TiO_2 were below 40 m^2 g^{-1}. The powder X-ray diffractograms show the reflexes of Ag as well as those of the support. Due to the amorphous nature of γ-Al_2O_3 and SiO_2, broad peaks were present, while sharp narrow lines were observed for crystalline MgO, TiO_2 and ZnO (Fig. S1†). Using the Scherrer equation, the silver crystallites were estimated to be ~27 and 40 nm on SiO_2 and γ-Al_2O_3, respectively. On supports that had a smaller specific surface area, the silver agglomerated and the particles grew to a size of 63 to 114 nm.

As the silver loading on the γ-Al_2O_3 increased, both the surface area and pore volume decreased (Table 1). However, even at 20 wt% Ag, the sample still had a surface area of 114 m^2 g^{-1}. The pore size distribution of the samples was rather wide, ranging from around 3 to 7 nm, with the average pore diameter at 4.6 nm. Despite increasing the silver loading, the pore size distribution of the supported samples remained similar to that of the γ-Al_2O_3 support (Fig. S2†). Diffraction peaks of metallic silver were observed in the powder X-ray diffractograms (XRD) of the Al_2O_3-supported samples with 5 to 20 wt% loading (Fig. S3†). The crystallite size increased with loading from 5 to 93 nm. From transmission electron microscopy (TEM), the metal particles showed a broad size distribution with the average crystallite size being smaller than that obtained from XRD (Fig. S4†). This discrepancy could be due to the smaller sampling size in TEM than in XRD.

To examine the oxidation state of surface silver atoms on the supported catalysts, XPS line positions for the 5–20 wt% Ag/Al_2O_3 catalysts were determined (Fig. S5†). The difference in the chemical shift for Ag(0) and Ag(I) is small and not unambiguous. Furthermore, with sample charging, it is difficult to accurately distinguish between the different oxidation states of silver.[26,27] Hence, the modified Auger parameter, α', which is the sum of the binding energy of the Ag $3d_{5/2}$ photoelectron and the kinetic energy of the Ag M_4VV Auger electron, is used instead. The value of α' is independent of any chemical shifts due to surface charging as the shifts in the binding energy (BE) and kinetic energy (KE) are of the same magnitude but in opposite directions.[28] The α' value lies between 722.68 and 723.99 eV (Table 2), which is in the range of Ag_2O, while metallic Ag is expected at ~726 eV.[29,30] The formation of an oxidized surface overlayer is not unexpected as the samples have been calcined in air at 500 °C. However, as observed from the XRD spectra, the bulk of the silver is in the metallic form. The Ag/Al ratio as deduced by XPS is higher than that expected from the loading. This is due to the method of catalyst preparation where silver was impregnated onto the Al_2O_3 support, resulting in a high concentration of the metal at the surface of the catalyst particles.

3.2 Catalytic studies

3.2.1 Optimization of reaction conditions. Silver supported on ZnO or MgO (Table 3, entries 2 & 3) was inactive for the protodecarboxylation of 2-nitrobenzoic acid to nitrobenzene. In contrast, when silver was supported on SiO_2, TiO_2 or Al_2O_3, the conversion was between 65 and 81% after 16 h (Table 3, entries 4–6). No conversion was observed over the alumina support alone.

Using 10 wt% Ag/Al_2O_3 as the standard catalyst, the reaction was optimized by varying the additives and solvent used.

Table 2 XPS results for Ag/Al_2O_3

Ag (wt%)	BE Ag $3d_{5/2}$ (eV)	KE Ag $M_4N_{45}N_{45}$ (eV)	α'-Parameter (eV)	Ag/Al XPS	Ag/Al Expected
5	367.05	356.21	723.26	0.04	0.03
10	367.20	356.54	723.74	0.09	0.05
15	367.25	355.43	722.68	0.14	0.08
20	367.40	356.59	723.99	0.18	0.12

Table 3 Influence of support, base and solvent on activity

Entry	Catalyst	Solvent	Additive	Temp. (°C)	Conv. (%)
1	Al_2O_3	NMP	K_2CO_3	120	0
2	10 wt% Ag/ZnO	NMP	K_2CO_3	120	0
3	10 wt% Ag/MgO	NMP	K_2CO_3	120	0
4	10 wt% Ag/SiO_2	NMP	K_2CO_3	120	80
5	10 wt% Ag/TiO_2	NMP	K_2CO_3	120	65
6	10 wt% Ag/Al_2O_3	NMP	K_2CO_3	120	81
7	10 wt% Ag/Al_2O_3	NMP	—	120	5.9
8	10 wt% Ag/Al_2O_3	NMP	AcOH	120	5.6
9	10 wt% Ag/Al_2O_3	DMF	K_2CO_3	120	38
10	10 wt% Ag/Al_2O_3	DMSO	K_2CO_3	120	76
11	10 wt% Ag/Al_2O_3	DMA	K_2CO_3	120	93
12	10 wt% Ag/Al_2O_3	Dioxane	K_2CO_3	101	5.0
13	10 wt% Ag/Al_2O_3	Toluene	K_2CO_3	111	20
14[a]	10 wt% Ag/Al_2O_3	DMA	K_2CO_3	120	86
15[b]	10 wt% Ag/Al_2O_3	DMA	K_2CO_3	120	93
16	Ag (ex-Ag_2CO_3)	DMA	K_2CO_3	120	7.5
17	Ag_2O (ex-Ag_2CO_3)	DMA	K_2CO_3	120	23
18	Ag (commercial)	DMA	K_2CO_3	120	0.9
19	Ag_2O (commercial)	DMA	K_2CO_3	120	35

Reaction conditions: 2 mmol 2-nitrobenzoic acid, catalyst (0.2 mmol Ag), 15 mol% K_2CO_3, 4 mL solvent, 120 °C, 16 h.[a] Pretreatment in flowing H_2 at 300 °C for 0.5 h before use. [b] Recycled catalyst.

The presence of a base, *e.g.*, K_2CO_3, was necessary to obtain a high conversion. Without the base, the conversion remained below 6% (Table 3, entries 7 & 8).

Different solvents were tested for the reaction, and polar aprotic solvents were found to favour the reaction (Table 3, entries 9–13). In solvents such as dimethyl sulfoxide (DMSO), dimethylacetamide (DMA) and NMP, conversions of 76–93% were obtained. The lone pairs of electrons on the oxygen, nitrogen or sulfur atoms allow these solvents to form σ-bond with the silver species. Furthermore, the oxygen atom can also act as a π-donor. The formation of the σ- and π-bond as well as the donation of electrons into the empty bonding d-orbitals of silver lower the energy level and stabilize the metal centre, thereby increasing its catalytic activity.

Unexpectedly, hydrogen pretreatment had a negative effect on the activity of the catalyst. After reduction of the 10 wt% Ag/Al_2O_3 catalyst at 300 °C under flowing hydrogen for 0.5 h, the initial rate of reaction was low, and the conversion after 1 h in air was only 10% as compared to 75% for the unreduced catalyst (Fig. 1). The better activity of the latter suggests that Ag^+ ions are important for decarboxylation. Indeed, the conversion over the reduced catalyst increased slowly over time to reach 86% after 5 h (Table 3, entry 14). As the reaction was conducted in a system open to the environment, diffusion of air could have led to reoxidation of the metallic silver catalyst and consequently, the formation of a more active catalyst. Indeed, when the reaction was conducted under N_2 using the reduced Ag catalyst, the lack of O_2 prevented the reoxidation of the catalyst, resulting in almost no conversion. In comparison, use of the unreduced Ag catalyst in the inert N_2 atmosphere had no adverse effect on the rate of the reaction, and the kinetic profile was similar to that for the reaction in air (Fig. 1).

3.2.2 Effect of particle size on activity. The influence of particle size on the protodecarboxylation of 2-nitrobenzoic acid was studied at 120 °C. The quantity of catalyst was adjusted so that the same amount of silver was used in each reaction. The initial rate of reaction (integrated over the first hour) increased from 5.1 to 7.6 mmol $mmol_{Ag}^{-1}$ h^{-1} for a silver loading of 5 and 10 wt%, respectively (Table S1†). Beyond this loading, the rate fell.

To elucidate the efficiency of the supported silver catalyst as a function of metal loading, the turnover frequency (TOF) was calculated as function of the number of external surface atoms available for reaction, $N_{s,rxn}$ (ESI†). This number was estimated based on the mean crystallite size.[31,32] The number of surface atoms available for reaction decreased with increasing silver content (Table S1†). This decrease is most drastic when the metal loading changed from 5 to 10 wt% where an eight-fold increase in the crystallite size from 5 to 40 nm was observed. However, the TOF based on the number of silver atoms at the surface increased from 19.6 h^{-1} for 5 wt% Ag/Al_2O_3 to a maximum of 216 h^{-1} for the 10 wt% Ag/Al_2O_3 catalyst (Fig. 2). With even higher loading of 15 and 20 wt% Ag, the TOF decreased moderately to 173 and 125 h^{-1}, respectively. It finally reached a constant value of about 90 h^{-1} for the silver powders which had much larger particle sizes (2.2–22 μm) than the supported catalysts. The kinetic profiles show clearly that the supported catalyst (10 wt% Ag/Al_2O_3) has a far superior catalytic activity for the protodecarboxylation than any of the silver powders or bulk Ag_2O (Fig. 3). The initial rate for the Ag_2O catalysts was at least 9 to 15 times smaller than that of 10 wt% Ag/Al_2O_3. Thus, the supported catalyst does not only gain from the higher dispersion of the metal, but also shows some additional activation due to the support.

The results suggest that the protodecarboxylation of 2-nitrobenzoic acid is more facile over silver crystallites of

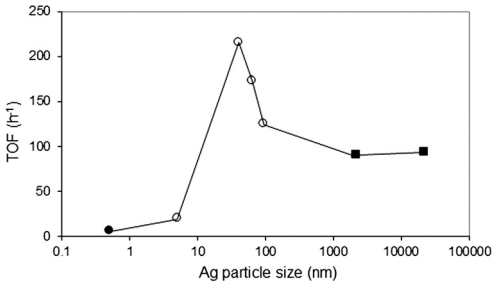

Fig. 2 TOF as a function of silver particle size for (○) Ag/Al_2O_3 and (■) Ag powder. (●) denotes homogeneous catalyst AgOAc.

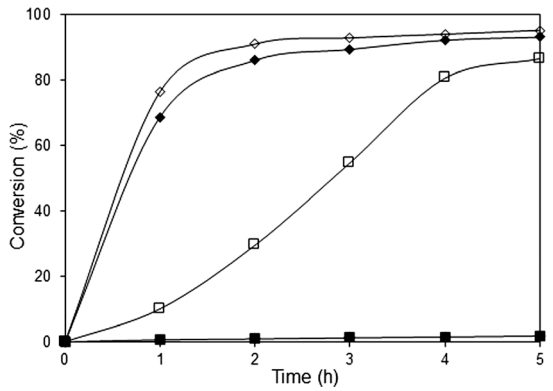

Fig. 1 Conversion of nitrobenzoic acid in air (open symbols) and N_2 (closed symbols) over 10 wt% Ag/Al_2O_3 calcined in air at 500 °C (◇, ◆) and after reduction in hydrogen at 300 °C for 0.5 h (□, ■).

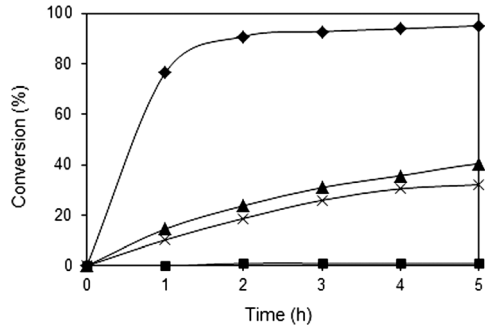

Fig. 3 Kinetic profiles for protodecarboxylation of 2-nitrobenzoic acid over (◆) 10 wt% Ag/Al_2O_3, (▲) Ag_2O (ex-Ag_2CO_3), (×) Ag_2O (commercial) and (■) Ag powder (ex-Ag_2CO_3).

bigger dimensions. As the crystallite size increases, the abundance of low coordination sites, *i.e.*, atoms at edges, steps and corners, decreases relative to those located at terraces or planes.[33,34] Hence, the reaction appears to take place preferentially at sites with higher coordination. This concept is further supported by the higher activity of 10 wt% Ag/Al_2O_3 compared with that of silver acetate. Silver acetate acts as a homogeneous catalyst as it dissolves in the hot acidic reaction medium. The initial rate of reaction for the heterogeneous 10 wt% Ag/Al_2O_3 catalyst was only slightly higher than for silver acetate, 7.6 *vs.* 6.2 mmol $mmol_{Ag}^{-1}$ h^{-1}. The difference in catalytic activity becomes much more significant when the comparison is made on the number of available silver ions. For the homogenous catalyst, this is all the silver added as silver acetate but for the heterogeneous catalyst, it is limited only to silver atoms at the external surface of the particles. The TOF is ~35 times higher for the heterogeneously catalyzed reaction than for the homogeneous system.

3.2.3 Role of the base. Various alkali metal carbonates such as Li_2CO_3, Na_2CO_3, K_2CO_3 and Cs_2CO_3 were tested under identical concentrations (15 mol% with respect to 2-nitrobenzoic acid). It is assumed that the alkali carbonate reacts with 2-nitrobenzoic acid, forming alkali 2-nitrobenzoate, CO_2 and water. Due to the limited amount of base (15 mol%), the reaction medium still contains some free acid. The activity for protodecarboxylation increased with the size of the alkali metal ions in the order Li < Na < K (Fig. 4). With K_2CO_3, the initial rate was 7.6 mmol $mmol_{Ag}^{-1}$ h^{-1} and 93% conversion was attained after 4 h. This may be due to an increase in base strength as the size of alkali metal ion increases. Furthermore, the degree of solvation is reduced for bigger cations, hence increasing their availability for reaction. However, with Cs_2CO_3 as the base, the conversion after 4 h was only 69.5%, with an initial rate of 1.41 mmol $mmol_{Ag}^{-1}$ h^{-1}. The low activity may be due to blockage of the active sites in the Ag_2O layer when the large cesium ion adsorbs onto the adjacent oxygen atom.

Reducing the amount of K_2CO_3 from 15 to 5 mol% decreased the initial rate by a factor of ten to 0.80 mmol $mmol_{Ag}^{-1}$ h^{-1}, and the conversion reached only 41% after 4 h (Table 4). A concentration of 15 mol% is optimum as increasing the K_2CO_3 amount beyond this gave lower activity (Fig. S6†).

The vast improvement in the conversion from 6 to 93% after the addition of 15 mol% K_2CO_3 suggests that either nitrobenzoate is the actual substrate, or potassium ions (K^+) play a role in modifying and activating the surface of the catalyst. To further understand the role of the base, the reaction was carried out starting with potassium nitrobenzoate (Table 5). A limiting conversion of 27% was reached after 4 h which can be attributed to a lack of protons within the system that prevents the formation of nitrobenzene after decarboxylation. This was confirmed because the conversion increased to 67% and 89% when the reaction was carried out in the presence of 15 and 100 mol% acetic acid, respectively. Hence, while the base is needed to generate the nitrobenzoate, the presence of both nitrobenzoate and 2-nitrobenzoic acid is necessary for the reaction.

An equivalent amount of KOH gave the same rate of reaction as K_2CO_3 (Fig. 5), showing that the rate was independent of the type of base. This is not surprising as in the presence

Table 4 Effect of amount of K_2CO_3 on the protodecarboxylation of 2-nitrobenzoic acid

K_2CO_3 (mol%)	Initial rate[a] (mmol $mmol_{Ag}^{-1}$ h^{-1})	Conversion[b] (%)
5	0.80	41
15	7.64	93
30	2.65	56
50	1.20	53

[a] Within 1 h. [b] After 4 h.

Table 5 Protodecarboxylation of 2-nitrobenzoic acid and potassium 2-nitrobenzoate under different conditions[a]

Entry	Substrate	K_2CO_3 (mol%)	AcOH (mol%)	Conversion (%)
1	2-Nitrobenzoic acid	—	—	6
2	2-Nitrobenzoic acid	15	—	93
3	Potassium 2-nitrobenzoate	—	—	27
4	Potassium 2-nitrobenzoate	—	15	67
5	Potassium 2-nitrobenzoate	—	100	89

[a] Reaction conditions: 2 mmol 2-nitrobenzoic acid, 10 wt% Ag/Al_2O_3 (0.2 mmol Ag), 15 mol% K_2CO_3, 4 mL DMA, 120 °C, 4 h.

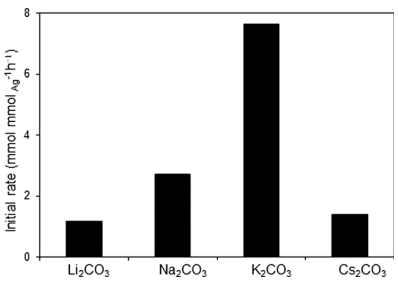

Fig. 4 Effect of different alkali metal carbonates on initial rate of protodecarboxylation of 2-nitrobenzoic acid.

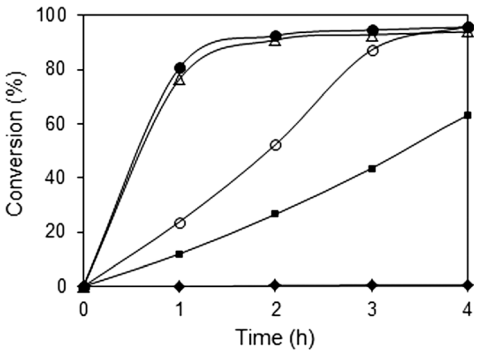

Fig. 5 Protodecarboxylation of 2-nitrobenzoic acid over 10 wt% Ag/Al_2O_3 in the presence of (◆) 0.3 mmol KCl (■) 0.3 mmol K_2SO_4 (△) 0.3 mmol K_2CO_3 (○) 0.3 mmol KOH and (●) 0.6 mmol KOH.

of excess 2-nitrobenzoic acid, there would be no K_2CO_3 or KOH present. To study if the K^+ ions play a role in the reaction, a neutral salt, K_2SO_4, was used instead of the base. A conversion of 62% was obtained after 4 h, showing that K^+ ions are important in the reaction. The rate of reaction is lower than with K_2CO_3, but this may be due to the limited solubility of K_2SO_4 in DMA. However, when KCl was used instead of K_2SO_4, no protodecarboxylation of 2-nitrobenzoic acid was observed, suggesting that the Cl^- reacted with the Ag_2O overlayer of the catalyst to form unreactive AgCl.

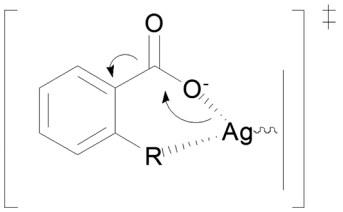

Scheme 2 *Ortho*-substituent coordinating to the Ag centre during decarboxylation.

3.3 Scope of reaction

The scope of the reaction was explored using various substituted aromatic carboxylic acids (Table 6). Benzoic acid did not undergo any protodecarboxylation. This is in contrast to the conversion of 93% observed with 2-nitrobenzoic acid and shows that an *ortho*-substituent must be present for protodecarboxylation to proceed in high yields over the heterogeneous Ag/Al_2O_3 catalyst. Although the *meta*-substituted 3-nitrobenzoic acid did undergo some protodecarboxylation, the conversion was only 15%. When two nitro groups are present at the *meta* positions, the conversion was higher, and 3,5-dinitrobenzoic acid could be decarboxylated with 52% yield. However, *para*-substituted 4-nitrobenzoic acid was not active towards protodecarboxylation. This agrees well with previous results by the groups of Gooßen[35] and Larrosa[16] who postulated that an intermediate is formed between the carboxylate group, the *ortho*-substituent and the metal center (Scheme 2). A similar complex can also form between an adsorbed benzoate anion and surface Ag^+ sites on the heterogeneous catalyst. An electron-withdrawing group at the *ortho* position can exert an inductive effect *via* the σ-backbone, favouring decarboxylation. This inductive effect decreases with increasing distance for substituents in *meta*- and *para*-positions.

Replacing the strongly electron withdrawing nitro group with a bromo group led to a lower conversion of 51% (Table 6, entry 7). Benzoic acids *ortho*-substituted with chloro or fluoro groups were highly active towards protodecarboxylation (Table 6, entries 8–10). While carboxylic acids with activating substituents such as methyl, hydroxyl, cyano and amino groups were inert to protodecarboxylation over our catalyst, good activity was observed for 2-methoxybenzoic acid. This may be due to coordination of the lone pair of electrons on the oxygen of the methoxy group to the metal center, thus stabilizing the intermediate formed during the decarboxylation step. Protodecarboxylation of heteroaromatic carboxylic acids also proceeded with high conversions (Table 6, entries 17–21). These results show that our heterogeneous Ag catalyst shows a similar performance to previously described homogeneous Ag catalysts,[15–17] where both can tolerate a range of substituents such as nitro, methoxy, bromo, chloro, fluoro groups as well as heteroaromatic carboxylic acids.

The reuse of the Al_2O_3-supported silver catalyst was studied. After the batch reaction, the catalyst was removed from

Table 6 Protodecarboxylation of various aromatic carboxylic acids over 10 wt% Ag/Al_2O_3

Entry	Substrate	Position of substituent	Effect of substituent	Conv.[a] (%)	Sel. (%)
1	Benzoic acid	—	—	0	—
2	2-Nitrobenzoic acid	*Ortho*	Strongly deactivating	93[b]	100
3	3-Nitrobenzoic acid	*Meta*	Strongly deactivating	15	100
4	4-Nitrobenzoic acid	*Para*	Strongly deactivating	0	—
5	3,5-Dinitrobenzoic acid	Di-*meta*	Strongly deactivating	52	100
6	4-Fluoro-2-trifluoromethylbenzoic acid	*Ortho*	Strongly deactivating	87	100
7	2-Bromobenzoic acid	*Ortho*	Weakly deactivating	51	100
8	2-Chlorobenzoic acid	*Ortho*	Weakly deactivating	89	100
9	2-Chloro-4-nitrobenzoic acid	*Ortho*	Weakly deactivating	99	100
10	2-Fluoro-4-chlorobenzoic acid	*Ortho*	Weakly deactivating	98	100
11	2-Toluic acid	*Ortho*	Weakly activating	0	—
12	2-Phenyl-benzoic acid	*Ortho*	Weakly activating	0	—
13	2-Methoxybenzoic acid	*Ortho*	Strongly activating	89	46
14	Salicylic acid	*Ortho*	Strongly activating	0	—
15	2-Cyanobenzoic acid	*Ortho*	Strongly activating	0	—
16	Anthranilic acid	*Ortho*	Strongly activating	0	—
17[c]	2-Picolinic acid	—	—	88	100
18[c]	2-Thiophenecarboxylic acid	—	—	100	100
19[c]	2-Furoic acid	—	—	98	100
20	2-Benzothiophene carboxylic acid	—	—	98	100
21	2-Benzofuran carboxylic acid	—	—	100	100

Reaction conditions: 2 mmol substrate, 10 wt% Ag/Al_2O_3 (0.2 mmol Ag), 15 mol% K_2CO_3, 4 mL DMA, 120 °C.[a] After 16 and. [b] 4 h. [c] Carried out in an autoclave as products have low boiling points.

the reaction mixture through centrifugation, and washed with DMA followed by water to remove any adsorbed organics and base residues, respectively. The recovered catalyst was dried in vacuum and recalcined at 500 °C for 1 h. The test results showed no significant loss in activity for the protodecarboxylation of 2-nitrobenzoic acid (Table 3, entry 15). The X-ray diffractogram of the recycled catalyst revealed no changes in the silver phase or Al_2O_3 support, indicating the stability of the alumina-supported Ag catalyst under the reaction conditions. Hence, this simple catalytic system offers ease of preparation, handling and reuse without needing other additives aside from K_2CO_3 for activity.

3.4 Reaction mechanism

Based on these results, a mechanism for the protodecarboxylation reaction is proposed (Scheme 3). In the presence of the base, *e.g.*, K_2CO_3, the free carboxylic acid is transformed to potassium nitrobenzoate. The observation that relatively large catalyst particles are required for good activity suggests that the substrate interacts with more than one Ag^+ site. The nitrobenzoate anion contains carboxylate and nitro groups which are electrostatically attracted to the positively charged Ag^+ ions at the Ag_2O surface layer. Decarboxylation of the 2-nitrobenzoate anion leads to a surface-bound negatively charged aryl–silver intermediate and the release of CO_2. A second incoming 2-nitrobenzoic acid molecule interacts with the neighbouring potassium ion *via* the oxygen of its carboxylic acid group, aiding in the deprotonation step. The released proton binds to the aryl–silver intermediate and forms the product, nitrobenzene. Upon desorption of nitrobenzene, the 2-nitrobenzoate anion adsorbs onto the catalyst surface for the next catalytic cycle. Hence, only a catalytic amount of the base is needed for the initial formation of the nitrobenzoate anion. The base can also be substituted by a neutral salt, *e.g.*, potassium sulphate, where the potassium ion facilitates the deprotonation of the 2-nitrobenzoic acid.

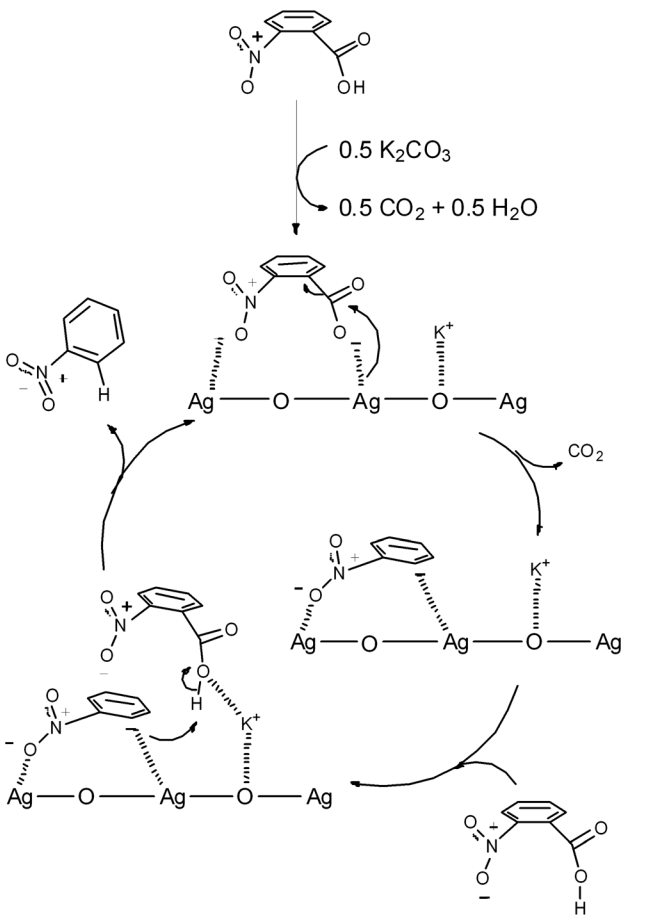

Scheme 3 Proposed catalytic cycle for the protodecarboxylation of *ortho*-substituted benzoic acid over an oxidized silver surface.

4. Conclusion

Silver supported on alumina and silica formed active catalysts for the protodecarboxylation of 2-nitrobenzoic acid. The activity for protodecarboxylation of 2-nitrobenzoic acid was maximal for 10 wt% Ag/Al_2O_3. The TOF for this catalyst, which contains silver particles of about 40 nm size, was 216 h^{-1}, which is much higher than that for the homogeneous silver acetate catalyst (TOF 6.2 h^{-1}) and also higher than metallic silver powder (90 h^{-1}). XPS revealed that the silver catalyst was covered by a surface layer of silver oxide, Ag_2O. The silver oxide layer, polar aprotic solvents such as DMSO, DMA or NMP, and a base are all required for high activity. In the presence of the base, 2-nitrobenzoic acid forms 2-nitrobenzoate. The presence of both acid and salt is required for reaction. Mechanistic studies indicate that the catalytic cycle involves the interaction of substrate molecules with more than one Ag^+ site. This explains the need for an extended catalytic site, and the fact that moderately large metal particles (*ca.* 40 nm) give the highest catalytic activity.

Acknowledgements

Financial support from National University of Singapore under grant numbers R-143-000-418-112 and R-143-000-476-112 is gratefully acknowledged.

Notes and references

1 L. J. Goossen, F. Collet and K. Goossen, *Isr. J. Chem.*, 2010, **50**, 617.
2 N. Rodriguez and L. J. Goossen, *Chem. Soc. Rev.*, 2011, **40**, 5030.
3 R. Shang and L. Liu, *Sci. China: Chem.*, 2011, **54**, 1670.
4 A. F. Shepard, N. R. Winslow and J. R. Johnson, *J. Am. Chem. Soc.*, 1930, **52**, 2083.
5 M. Nilsson, *Acta Chem. Scand.*, 1966, **20**, 423.
6 A. Cairncross, J. R. Roland, R. M. Henderson and W. A. Sheppard, *J. Am. Chem. Soc.*, 1970, **92**, 3187.
7 T. Cohen, R. W. Berninger and J. T. Wood, *J. Org. Chem.*, 1978, **43**, 837.
8 L. J. Goossen, W. R. Thiel, N. Rodriguez, C. Linder and B. Melzer, *Adv. Synth. Catal.*, 2007, **349**, 2241.

9 L. J. Goossen, F. Manjolinho, B. A. Khan and N. Rodriguez, *J. Org. Chem.*, 2009, **74**, 2620.
10 M. Rudzki, A. Alcalde-Aragonés, W. I. Dzik, N. Rodríguez and L. J. Gooßen, *Synthesis*, 2012, 184.
11 J. S. Dickstein, C. A. Mulrooney, E. M. O'Brien, B. J. Morgan and M. C. Kozlowski, *Org. Lett.*, 2007, **9**, 2441.
12 Z. M. Sun and P. Zhao, *Angew. Chem., Int. Ed.*, 2009, **48**, 6726.
13 S. Dupuy, F. Lazreg, A. M. Z. Slawin, C. S. J. Cazin and S. P. Nolan, *Chem. Commun.*, 2011, **47**, 5455.
14 J. Cornella, M. Rosillo-Lopez and I. Larrosa, *Adv. Synth. Catal.*, 2011, **353**, 1359.
15 L. J. Goossen, C. Linder, N. Rodriguez, P. P. Lange and A. Fromm, *Chem. Commun.*, 2009, 7173.
16 J. Cornella, C. Sanchez, D. Banawa and I. Larrosa, *Chem. Commun.*, 2009, 7176.
17 P. Lu, C. Sanchez, J. Cornella and I. Larrosa, *Org. Lett.*, 2009, **11**, 5710.
18 J. Hagen, *Industrial Catalysis*, Wiley-VCH, Weinheim, 2006, pp. 99–222.
19 A. M. Ruppert and B. M. Weckhuysen, in *Handbook of Heterogeneous Catalysis*, ed. G. Ertl, H. Knözinger, F. Schüth, and J. Weitkamp, Wiley-VCH, Weinheim, 2008, vol. 3, pp. 1178–1188.
20 A. T. Bell, *Science*, 2003, **299**, 1688.
21 H. Einaga and A. Ogata, *Environ. Sci. Technol.*, 2010, **44**, 2612.
22 K.-I. Shimizu, M. Tsuzuki, K. Kato, S. Yokota, K. Okumura and A. Satsuma, *J. Phys. Chem. C*, 2006, **111**, 950.
23 K. Shimizu, K. Shimura, M. Nishimura and A. Satsuma, *ChemCatChem*, 2011, **3**, 1755.
24 G. J. K. Acres, A. J. Bird, J. W. Jenkins and F. King, in *Catalysis*, ed. C. Kemball and D. A. Dowden, The Royal Society of Chemistry, London, 1981, vol. 4, pp. 1–30.
25 A. L. Patterson, *Phys. Rev.*, 1939, **56**, 978.
26 M. Richter, M. Langpape, S. Kolf, G. Grubert, R. Eckelt, J. Radnik, M. Schneider, M. M. Pohl and R. Fricke, *Appl. Catal., B*, 2002, **36**, 261.
27 G. B. Hoflund and Z. F. Hazos, *Phys. Rev. B: Condens. Matter Mater. Phys.*, 2000, **62**, 11126.
28 S. W. Gaarenstroom and N. Winograd, *J. Chem. Phys.*, 1977, **67**, 3500.
29 C. D. Wagner and A. Joshi, *J. Electron Spectrosc. Relat. Phenom.*, 1988, **47**, 283.
30 D. Briggs, in: *Handbook of X-ray Photoelectron Spectroscopy* ed. C. D. Wanger, W. M. Riggs, L. E. Davis, J. F. Moulder and G. E. Muilenberg, Perkin-Elmer Corp., Physical Electronics Division, Eden Prairie, Minnesota, USA, 1979, pp. 120–121.
31 A. Abad, A. Corma and H. García, *Chem.–Eur. J.*, 2008, **14**(1), 212.
32 R. E. Benfield, *J. Chem. Soc., Faraday Trans.*, 1992, **88**, 1107.
33 A. M. Doyle, S. K. Shaikhutdinov and H.-J. Freund, *Angew. Chem., Int. Ed.*, 2005, **44**, 629.
34 A. Corma, P. Serna, P. Concepción and J. J. Calvino, *J. Am. Chem. Soc.*, 2008, **130**, 8748.
35 L. J. Gooßen, N. Rodríguez, C. Linder, P. P. Lange and A. Fromm, *ChemCatChem*, 2010, **2**, 430.